

Lawrence Berkeley National Laboratory

Recent Work

Title

TIME-OF-FLIGHT PHOTOELECTRON SPECTRO-SCOPY OF GASES USING SYNCHROTRON RADIATION

Permalink

<https://escholarship.org/uc/item/02d599mc>

Author

White, M.G.

Publication Date

1979-03-01

TIME-OF-FLIGHT PHOTOELECTRON SPECTROSCOPY OF
GASES USING SYNCHROTRON RADIATION

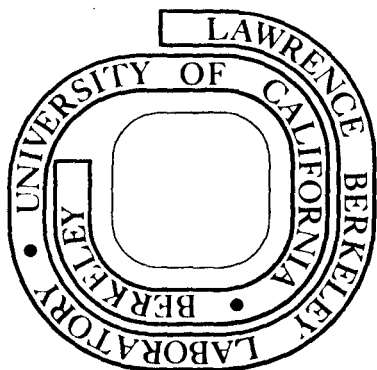
M. G. White, R. A. Rosenberg, G. Gabor, E. D. Poliakoff,
G. Thornton, S. H. Southworth, and D. A. Shirley

March 1979

Prepared for the U. S. Department of Energy
under Contract W-7405-ENG-48

TWO-WEEK LOAN COPY

*This is a Library Circulating Copy
which may be borrowed for two weeks.
For a personal retention copy, call
Tech. Info. Division, Ext. 6782*



RECEIVED
LAWRENCE
BERKELEY LABORATORY

MAY 8 1979

LIBRARY AND
DOCUMENTS SECTION

LBL-8851 c.2

DISCLAIMER

This document was prepared as an account of work sponsored by the United States Government. While this document is believed to contain correct information, neither the United States Government nor any agency thereof, nor the Regents of the University of California, nor any of their employees, makes any warranty, express or implied, or assumes any legal responsibility for the accuracy, completeness, or usefulness of any information, apparatus, product, or process disclosed, or represents that its use would not infringe privately owned rights. Reference herein to any specific commercial product, process, or service by its trade name, trademark, manufacturer, or otherwise, does not necessarily constitute or imply its endorsement, recommendation, or favoring by the United States Government or any agency thereof, or the Regents of the University of California. The views and opinions of authors expressed herein do not necessarily state or reflect those of the United States Government or any agency thereof or the Regents of the University of California.

Time-of-Flight Photoelectron Spectroscopy of
Gases Using Synchrotron Radiation

M. G. White, R. A. Rosenberg, G. Gabor,
E. D. Poliakoff, G. Thornton,
S. H. Southworth, and D. A. Shirley

Materials and Molecular Research Division
Lawrence Berkeley Laboratory
and
Department of Chemistry
University of California
Berkeley, California 94720

March 1979

ABSTRACT

A gas-phase time-of-flight (TOF) photoelectron spectrometer has been developed for use with synchrotron radiation. The excellent time structure of the synchrotron radiation at the Stanford Positron Electron Accelerator Ring (SPEAR) has been used as the time base for the TOF measurements. The TOF analyzer employs two multichannel plates (MCP's) in tandem as a fast electron multiplier with a matched 50 Ω anode to form an electron detector with a timing resolution of ≤ 70 psec. The spectrometer is presently capable of analyzing electrons over a wide energy range (1 eV to 50 eV) at medium energy resolution ($\leq 5\%$) and high angular resolution ($\pm 3^\circ$).

I. INTRODUCTION

The unique features of synchrotron radiation as a vacuum ultraviolet (VUV) light source offer tremendous advantages over laboratory sources for the study of photoionization processes in atoms and molecules. The tunability and high degree of linear polarization of synchrotron radiation allows the study of photoionization cross sections and angular distributions over a wide range of electron kinetic energies. Such data are particularly useful for the critical evaluation of theoretical models describing the interactions between the ion core and the continuum electron. In addition, direct resonant excitation to highly excited Rydberg levels of the neutral species (which subsequently autoionize into the ionization continuum) is made possible. Thus the basic electronic structure of these Rydberg levels and their coupling to the excited ionic states can be investigated directly.

Photoelectron spectroscopy of gases using present day synchrotron radiation sources, however, is a comparatively low counting rate experiment. This is a result of both the relatively small photon fluxes available in the VUV (typically $<10^{11} \text{ sec}^{-1} \text{ cm}^{-2}$) and the small sample densities ($<10^{14} \text{ cm}^{-3}$) normally employed in gas-phase photoelectron measurements. Also, angle-resolved experiments require an angular resolution of at least $\pm 5^\circ$, implying a collection solid angle of $\leq 10^{-2}$ steradians. These factors lead to typical counting rates of $10 - 100 \text{ sec}^{-1}$, depending on the cross section of the species being studied.

It is therefore imperative to develop very efficient electron analyzers to avoid prohibitively long counting times. To date nearly all gas-phase photoelectron experiments using synchrotron radiation have employed electrostatic deflection electron analyzers, either a 127° cylindrical mirror sector¹ or a cylindrical mirror analyzer.² Although these analyzers have high resolving capabilities, they are intrinsically inefficient because electrons in only a narrow energy range are collected at any one time.

An alternative and much more efficient method of electron kinetic energy analysis is by the time-of-flight (TOF) technique. A TOF analyzer measures the time required for a photoelectron to travel over a fixed distance of field free space after an ionizing event. Using standard timing/coincidence techniques, TOF analysis permits the entire energy spectrum within a given time window to be analyzed simultaneously. The counting efficiency is therefore increased relative to the more conventional deflection-type analyzers by a factor equal to the number of collecting channels (typically 10^3). Since all the peaks in a given spectrum are collected simultaneously it is not necessary to normalize relative peak areas for fluctuations in sample pressure and beam decay. In addition, because TOF is a coincidence technique, random background contributions such as electron multiplier dark noise are equally divided among the time channels of a collection window which includes the entire repetition period of the pulsed source.

Hence, the background contribution to any given time channel is significantly reduced and signal-to-background ratios of 1:1 or smaller can be tolerated. Because the actual collection time window is normally smaller than the full repetition period, a further improvement in the total signal-to-background ratio is obtained.

In practice, TOF analysis requires either a pulsed radiation source or, in the case of continuous excitation, that the electrons be pulsed from the interaction region by applied external fields. The latter approach suffers from the disadvantages that photoelectrons are produced continuously, introducing additional background and broadening of peaks and that the collection solid angle varies with electron kinetic energy. Unfortunately, with laboratory photon sources in the VUV it is generally not feasible to attain the repetition frequencies (≥ 10 KHz) and small pulse widths (≤ 1 nsec) necessary for optimal electron TOF measurements. The pulsed nature of synchrotron radiation from large storage rings, however, provides an ideal time base for electron TOF analysis. Recently, Bachrach, et al.,³ performed solid state photoemission experiments employing a prototype TOF analyzer and the pulsed synchrotron radiation at the Stanford Positron Electron Accelerator Ring (SPEAR). These measurements clearly established the feasibility and usefulness of the TOF technique based on pulsed synchrotron radiation.

In this paper we discuss the design of a new gas phase photoelectron spectrometer employing a TOF electron energy analyzer. TOF detection is facilitated by the excellent time structure (0.3 nsec pulse width and a 780 nsec repetition period) of the radiation produced at SPEAR. These timing characteristics are ideal for electron TOF analysis because the very narrow pulse imparts only a small kinetic energy spread to the ejected electrons (40 meV at 10 eV). Furthermore, the relatively long repetition period permits kinetic energies from 1 eV to several hundred eV to be analyzed using practical drift tube lengths (~ 30 cm).

The TOF apparatus described here is significantly different from other gas-phase TOF instruments using VUV radiation recently developed by Tsai, et al.,⁴ and Guyon, et al.⁵ In those spectrometers only near-threshold (≤ 1 eV) photoelectrons are detected, and they are collected over large solid angles, yielding spectra which are somewhat angle-integrated. These limitations would preclude certain studies of autoionization phenomena and photoelectron anisotropies. Because synchrotron radiation is ideally suited for probing resonant phenomena and angular distributions, our TOF detector was designed to analyze electrons over a wide energy range at medium energy resolution and high angular resolution.

The spectrometer is described in Section II. Its performance is discussed in Section III and projected future modifications are outlined in Section IV.

II. APPARATUS

The TOF apparatus shown schematically in Fig. 1 was designed for experiments on the 8° beam line at the Stanford Synchrotron Radiation Laboratory (SSRL). A detailed description of this facility is given elsewhere.⁶ Briefly, 3.2 milliradians of radiation from the storage ring is subtended by a mirror and focused onto the grating of 1-meter Seya-Namioka monochromator (GCA/McPherson). The radiation entering the sample chamber is 97% polarized in the horizontal plane. Photon energies of between 4 eV and 36 eV are available with the optics presently employed on the 8° line.

After final focusing, the beam passes through the window isolation fore chamber located between two pneumatically operated gate valves (Torr Vacuum). This section of the apparatus is used to isolate the sample chamber, which is operated at a relatively high pressure of $\sim 2 \times 10^{-5}$ torr, from the monochromator and beam line in which pressures below 10^{-9} torr are maintained. Isolation is accomplished by ultra-thin ($\sim 1500\text{\AA}$) In and Al windows which are capable of withstanding differential pressures of up to 1 torr and have acceptable transmission for the photon energies of interest (see Fig. 2).⁷ At the peak transmittance wavelength, $\sim 570\text{\AA}$, the photon flux is estimated to be $5 \times 10^9 \text{ sec}^{-1} \text{ cm}^{-2}$ for typical operating conditions of 2Å band pass and 10 mA SPEAR electron ring current. A sodium salicylate scintillator and optical phototube (RCA, 8850) are used to continuously monitor the beam intensity.

The gas sample enters the vacuum chamber through a disc of 10 μ diameter, 1 mm long microchannels (Galileo Corp.) sealed with epoxy to the end of a 1 mm capillary tube and located approximately 5 mm above the interaction region. After assembly, the inlet probe including the capillary array was vacuum coated with gold in order to prevent charging near the ionization region. The microchannel array serves to collimate the gas source, increasing the forward intensity over that of a simple effusive source of the same backing pressure. Based on the work of Johnson, et al.,⁸ and Jones, et al.,⁹ we estimate the increase in forward intensity, the "peaking factor",⁹ to be ~ 7 for a 5 torr backing pressure with a half-intensity beam angle of $\theta_{\frac{1}{2}} = 6.5^\circ$. Here $\theta_{\frac{1}{2}}$ is defined by $I(\theta_{\frac{1}{2}})/I(0^\circ) = \frac{1}{2}$. This can be compared to the 60° half intensity angle of an effusive beam source, indicating that significant collimation is achieved by expansion through the channel array. Backing pressures typically ranged between 2 torr and 10 torr as measured by a capacitance manometer (MKS Instruments, Inc.). At these backing pressures, the particle density is predicted to be $\sim 10^{13} \text{ cm}^{-3}$, which is consistent with the observed photoelectron counting rates. The resultant gas jet is directed into a conical "gas catch" directly below the ionization region which is pumped by a 500 liter/sec. turbomolecular pump (Airco-Temesal). A second 500 liter/sec. turbomolecular pump attached to the main chamber provides a background pressure of $\sim 2 \times 10^{-5}$ torr.

Photoelectrons enter the TOF analyzer through a 2.4 mm orifice located 2.3 cm from the center of the interaction region. The orifice collimates the ejected electron signal and also acts as a conduction barrier between the sample chamber and detector housing for the purpose of differential pumping. A total flight path of 28.5 cm was chosen to give an angular acceptance of $\pm 3^\circ$ and is limited by the diameter of the active area of the electron detector (2.84 cm). This angular resolution represents a compromise between limiting the variation in electron flight paths, which degrades the overall energy resolution, and insuring a sufficient collection solid angle (8.6×10^{-3} sr). Typical flight times for this distance are 480 nsec and 96 nsec for 1 eV and 25 eV electrons, respectively.

The drift tube is constructed from aluminum and provides the electrostatic shield for the field free flight path. The entire flight tube as well as the detector assembly is gold plated to eliminate contact potentials. In addition, the inside of the drift tube was coated with a colloidal graphite spray to reduce secondary electron emission caused by photoelectrons striking the walls of the shield. Magnetic shielding was provided by a coaxial μ -metal cylinder mounted around the flight tube. The residual magnetic field inside the drift space was measured to be less than 10 milligauss.

The electron amplifier is a tandem pair of microchannel plates (MCP) whose output is collected on a conical anode (Fig. 3). The MCP amplifier is similar in design to those recently employed for fast timing measurements of nuclear particles¹⁰ and heavy ions^{11,12} and the TOF electron detectors of Kennerly¹³ and Bachrach, et al.³ The general operating characteristics of MCP's and their timing capabilities have been discussed in detail in the literature cited above and hence will not be repeated here. It is sufficient to note that because of the small time dispersion in a MCP's amplifying process, single particle events can be timed with a resolution of <100 psec.

The electrons which have drifted through the field free region are accelerated by 100 V before impinging on the first MCP. The MCP's electron detection efficiency is >96% and is uniform for input kinetic energies of 100 eV to 700 eV.¹⁴ Two MCP's (Varian Series 8900, 40 mm diameter, 8° bias angle) in a Chevron arrangement were employed as the subnanosecond amplifier with up to 10^7 gain. Bias voltages from a divider chain (shown schematically in Fig. 3) were applied to the front and rear conducting surfaces of each MCP through .05 mm thick gold-plate brass rings. The contact rings between the two MCP's were isolated by a .05 mm Mylar spacer, giving a total separation of .15 mm between the two MCP's. The emerging electron cascade is collected on a coaxial anode whose surface diameter (2.84 cm) determines the useful active area

of the detector. The coaxial anode cone is designed to have the impedance of the anode increase from a minimum value of 16Ω at the collection surface to the output impedance of 50Ω . In this way a larger collection surface area is possible for a given MCP geometry than with a coaxial design in which the entire anode is fixed at 50Ω impedance. The anode shield is coupled to the back surface of the second MCP by a capacitor made from .5 mm double faced printed circuit board. The anode is at a virtual ground with respect to the anode shield, but the whole anode assembly is floated at the full positive high voltage potential. A fast coaxial transformer decouples the output signal to ground reference before passing through a high vacuum floating-shield coaxial BNC feedthrough (Ceramaseal, Inc.).

At an applied voltage of 2.5 kV, the detector provides a gain of 10^6 and a dark noise count rate of $1 - 10 \text{ sec}^{-1}$. The output pulses are very sharp, with a 10%-90% rise time of $\leq .5 \text{ nsec.}$ and pulse amplitudes of $\sim 75 \text{ mV.}$

Photoelectron spectra are generated by using the photon-electron coincidence counting circuit shown schematically in Fig. 3. Pulses from the electron multiplier are amplified and discriminated, then used as a start signal for a time-to-amplitude converter (TAC). The stop pulse is provided by a signal from an induction coil located in the storage ring. This arrangement of stop and start signals avoids reset-time losses in the TAC. The pulse-height spectrum is then analyzed and accumulated in a multichannel analyzer.

III. PERFORMANCE

The energy resolution for TOF analysis is given by¹⁵

$$\left(\frac{\Delta E}{E}\right)_{\text{TOF}} = \sqrt{\left(\frac{2\Delta t}{t}\right)^2 + \left(\frac{2\Delta \ell}{\ell}\right)^2} \quad (1)$$

where Δt and $\Delta \ell$ represent the total time resolution of the apparatus and the electron flight path uncertainty, respectively. The time resolution of the TOF detector system is determined by the timing capabilities of the electron multiplier and associated electronics, folded together with the time width of the synchrotron beam pulse. Timing dispersion in the MCP amplifier and electronics is <70 psec. and the width (FWHM) of the synchrotron radiation pulse varies from 150 psec. to 400 psec. depending on the operating conditions of SPEAR. Furthermore, the pulse shape is in general neither gaussian in time nor constant for different electron beam currents.¹⁶ The overall timing resolution of the apparatus was measured directly by the observation of prompt (Rayleigh) photon scattering from the gas sample. A prompt pulse is shown in Fig. 4. The measured FWHM of ~ 300 psec. leads to an energy resolution contribution from timing factors of 40 meV at 10 eV and represents the limiting resolution of our TOF apparatus when employed at SSRL.

Differences in the photoelectron flight paths ($\Delta \ell$) result from the finite source volume and finite collection solid

angle. The spread in electron flight paths due to the angular acceptance of $\pm 3^\circ$ contributes only a small energy uncertainty of .25%. A much larger contribution to $\Delta\ell$ results from the relatively large interaction volume from which the photoelectrons originate. With the present focusing optics on the 8° beam line, the photon beam cross section (FWHM) is 2.1 mm high by 4.2 mm wide at the interaction point. Furthermore, the experiments reported here were conducted at the "magic angle" (54.7° with respect to the photon polarization vector), hence, the horizontal beam profile at the source point is increased to ~ 7.3 mm. This would correspond to a $\sim 5\%$ resolution contribution if the electrons originated from the entire width of the beam. Due to the imperfect alignment of the photon beam and the highly collimated nature of the gas jet, however, the effective size of the interaction region is actually smaller. Hence, the 5% contribution represents an upper limit to the flight path uncertainty. Since this dispersion dominates the first term of Eq. (1) the energy resolution ($\Delta E/E$) is essentially constant over the kinetic energy range of 1 eV to 25 eV.

Although it is possible to use space focusing to reduce or eliminate the energy spread caused by the finite source width,¹⁵ the accompanying restrictions on the other design parameters of the TOF analyzer are severe. In the single acceleration field design, the length of the drift region is restricted to $\ell = 2s$ where s is the distance between the extraction elements. Hence, only near-threshold electrons can be analyzed, i.e., the first term in Eq. (1) is kept small.⁴ In

both the single and double accelerating field system described in Ref. 15, the electrons are extracted from the ionization region; hence, the effective angular acceptance of the analyzer is large and it varies with the kinetic energy of the electrons.

The total energy resolution is given by

$$\left(\frac{\Delta E}{E}\right)_{\text{TOTAL}} = \sqrt{\left(\frac{\Delta E}{E}\right)_{\text{TOF}}^2 + \left(\frac{\Delta \lambda}{\lambda}\right)^2} \quad (2)$$

where λ is the wavelength of the exciting radiation and $\Delta \lambda$ the monochromator band pass. The loss of intensity at higher resolution limited the usable band pass to 2.5\AA (~ 90 meV at 21.2 eV photon energy) in the work presented here.

The TOF photoelectron spectrum of the 5p shell of atomic Xe at $h\nu = 23.1$ eV is shown in Fig. 5. This spectrum was recorded in only 5 minutes and represents the time-to-energy converted raw data. The marked asymmetry of the peaks towards lower energies is again due to the "magic angle" geometry employed. This results in the analyzer accepting more electrons with longer flight paths and hence apparent lower kinetic energies.

The resolution of 4% found for the $^2P_{3/2}$ peak is smaller than predicted by Eqs. (1) and (2), presumably because of an over-estimation of the interaction source width as discussed above. A resolution of $\sim 4\%$ at 10 eV is comparable or better than that obtained with previous TOF electron analyzers. In the low energy (≤ 2 eV) electron spectrometers of Tsai, et al.,⁴

Land, et al.,¹⁷ Baldwin,¹⁸ and Wilden, et al.,¹⁹ energy resolutions ($\Delta E/E$) of 10% at 50 meV, 6% at 150 meV, 13% at 1 eV and 3.3% at 1 eV, respectively, were reported. Because the resolving capabilities of those spectrometers are limited by the time resolution of the detector (5-12 nsec), only the first term of Eq. (1), i.e., $\frac{2\Delta t}{t}$, contributes significantly to the energy resolution. Hence, ΔE is proportional to $E^{3/2}$ and their energy resolution will deteriorate rapidly with increasing kinetic energy. For detection of photoelectrons with energies greater than 1 eV, only the TOF apparatus of Kennerly¹³ has better resolution than the present spectrometer (.67% at 12 eV). The time dispersions in both spectrometers are essentially identical (300 psec.), however, a longer flight path (50 cm) and much smaller flight path uncertainty ($\Delta\ell = .1$ cm) significantly improves the overall energy resolution obtainable by Kennerly.

IV. FUTURE IMPROVEMENTS AND DEVELOPMENTS

By refocusing the photon beam as it exits the monochromator or decreasing the path length between the present final focusing mirror and the interaction region, it will be possible to reduce the beam cross section to a 2.2 mm \times 1.4 mm spot. This will reduce the path length dispersion, $\frac{2\Delta\ell}{\ell}$, from $\sim 5\%$ to 1.5%, resulting in a significant improvement in the overall energy resolution. In addition to reducing the beam size, a retarding grid assembly will also be added to the TOF analyzer. Retardation should provide a further improvement in the resolution, by simply reducing the field free kinetic energy. With

these modifications an energy resolution of $\Delta E \leq 100$ meV should be readily obtainable for photoelectron kinetic energies between 1 eV and 25 eV.

Future studies with the TOF apparatus include the measurement of electron angular distributions employing synchrotron radiation. The photoelectron angular distribution is completely characterized by the measurement of the asymmetry parameter, β , which is in turn determined by the transition strengths between the initial orbital and the dipole allowed final state continuum channels. The asymmetry parameter can vary rapidly with photon energy, particularly near the ionization threshold ($10 \text{ eV} < h\nu < 50 \text{ eV}$), making these experiments ideally suited for work on the 8° beam line at SSRL. The β measurements will be performed with this apparatus by collecting photoelectron spectra at two angles with two TOF analyzers. The spectrometer vacuum chamber has been designed to accept two analyzers at $\theta = 0^\circ$ and 90° with respect to the electric vector of the radiation so that the maximum change in the differential cross section can be exploited.²⁰ Using the input routing electronics shown in Fig. 6, the output of the two detectors can be analyzed with a single TAC and stored separately in a multichannel analyzer. Hence, photoelectron spectra at two different angles are collected simultaneously, allowing β for a particular photon energy to be computed from a single run. In this way the unique features of both synchrotron radiation and TOF energy analysis can be

fully utilized. This results in the most efficient and versatile experimental arrangement presently available for the study of photoelectron angular distributions of gases.

ACKNOWLEDGEMENT

This work is supported by the Division of Chemical Sciences, Office of Basic Energy Sciences, U.S. Department of Energy under contract No. W-7405-Eng-48.

REFERENCES

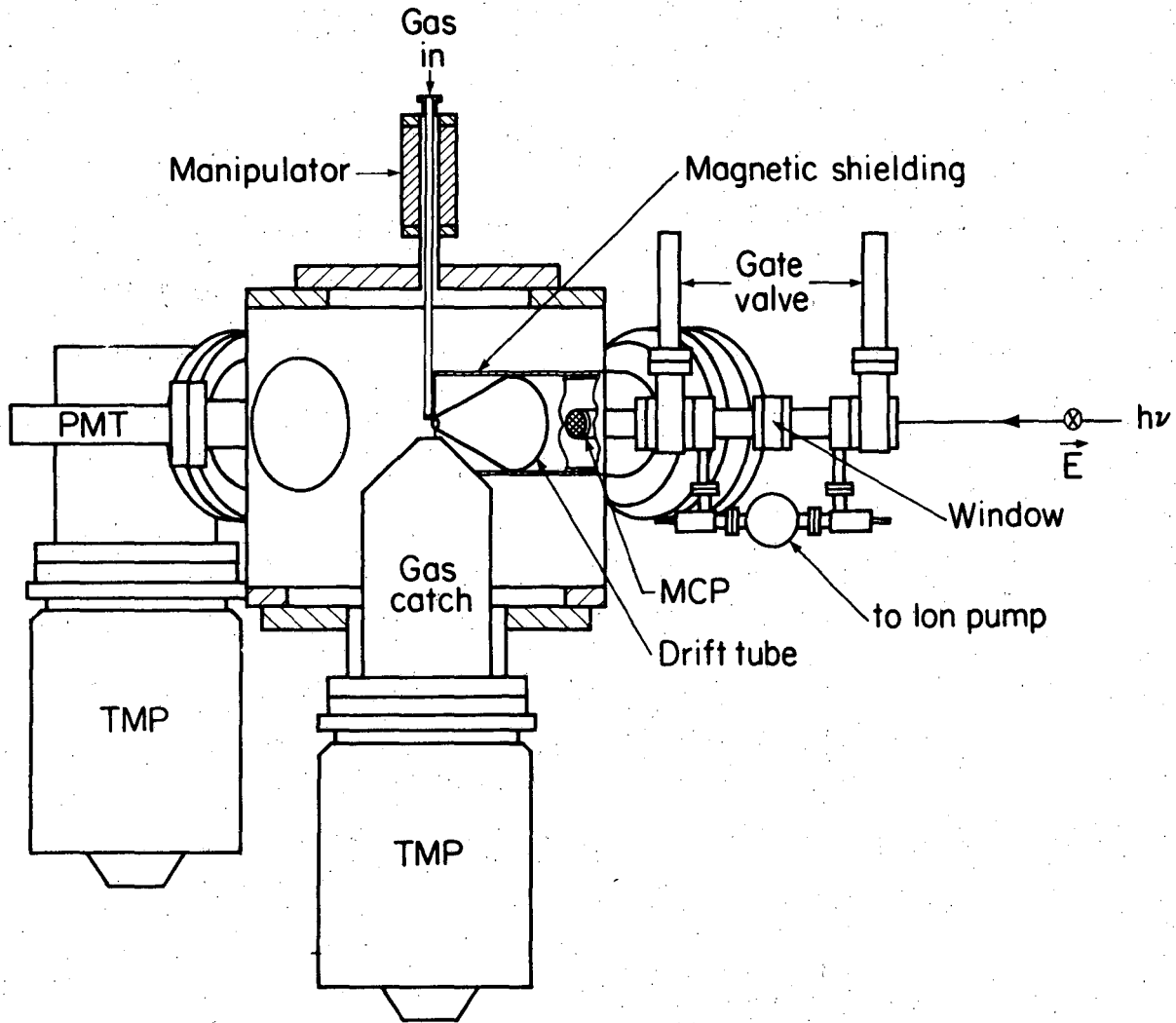
1. See for example, L. Torop, J. Morton, and J. B. West, J. Phys. B 9, 2035 (1976).
2. See for example, P. C. Kemeny, J.A.R. Samson, and A. F. Storace, J. Phys. B 10, L201 (1977).
3. R. Z. Bachrach, F. C. Brown, and S.B.M. Hagstrom, J. Vac. Sci. Tech. 12, 309 (1975).
4. B. Tasi, T. Baer, and M. L. Horowitz, Rev. Sci. Instrum., 45, 494 (1974).
5. P. M. Guyon, T. Baer, L.F.A. Ferreira, I. Nenner, A. Tabché-Fouhailés, R. Botter, and T. R. Govers, J. Phys. B 11, L141 (1978).
6. H. Winick, in VUV Radiation Physics, eds., E. E. Koch, et al. (Pergamon-Vieweg, London/Braunschweig, 1974), p. 780; V. Rehn, et al., in VUV Radiation Physics, eds., E. E. Koch, et al. (Pergamon-Vieweg, London/Braunschweig, 1974), p. 780.
7. Luxell Corporation, Santa Barbara, CA
8. J. C. Johnson, A. T. Stair, Jr., and J. L. Pritchard, J. Appl. Phys. 37, 1551 (1966).
9. R. H. Jones, D. R. Olander, and V. R. Kruger, J. Appl. Phys. 40, 4641 (1969).
10. M. I. Green, P. F. Kenealy, and G. B. Beard, Nucl. Instrum. and Methods 126, 175 (1975).
11. G. Gabor, W. Schimmerling, D. Greiner, F. Bieser, and P. Lindstrom, Nucl. Instrum. and Methods 130, 65 (1975).

12. J. Girard and M. Bolore, Nucl. Instrum. and Methods 140, 279 (1977).
13. R. E. Kennerly, Rev. Sci. Instrum. 48, 1682 (1977).
14. G. Gabor, to be published.
15. W. C. Wiley and I. H. McLaren, Rev. Sci. Instrum. 26, 1150 (1955).
16. A. P. Sabersky, in Abstracts of the Third Annual SSRP Users Group Meeting, Stanford, CA, 1976, p. 46.
17. J. E. Land and W. Raith, Phys. Rev. A9, 1592 (1974).
18. G. C. Baldwin, Phys. Rev. A9, 1225 (1974).
19. D. G. Wilden, P. J. Hicks, and J. Comer, J. Phys. B 9, 1959 (1976).
20. J.T.J. Huang, J. W. Rabalais, and F. O. Ellison, J. Electron Spectrosc. and Rel. Phen. 6, 85 (1975).

FIGURE CAPTIONS

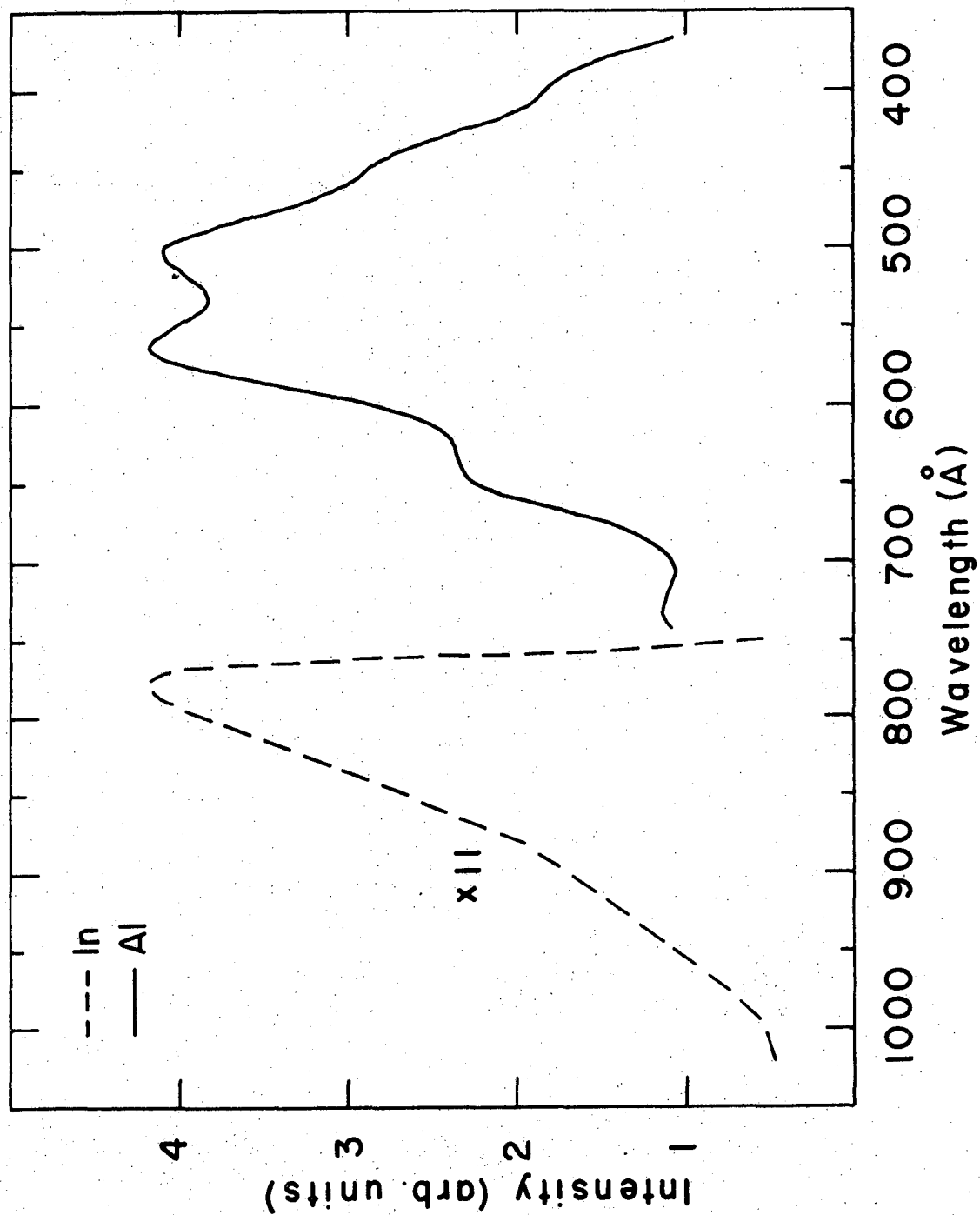
- Figure 1. Lay-out of the TOF photoelectron spectrometer. See text for detailed description.
- Figure 2. Relative transmitted intensity versus photon wavelength for the 8° beam line at SSRL employing In and Al windows.
- Figure 3. Schematic of the TOF analyzer and associated electronics. A = $1M\Omega$, B = $422k\Omega$, C = $1M\Omega$, D = $619k\Omega$, E = $750k\Omega$; the voltage divider and power supply were potted in thermally conducting epoxy and were heat sunk to the detector support stalk. MONO = 8° line monochromator. CS = ceramic spacer. MS = mylar spacer. MCP = 40 mm diameter microchannel plate. DC = decoupling capacitor. CA = coaxial anode. DT = decoupling transformer. CFD = constant fraction discriminator. Attn = 0-100 db. attenuator. DD = differential discriminator. TAC = time-to-amplitude converter. PHA/MCA = combination pulse height analyzer and multichannel analyzer.
- Figure 4. Prompt signal resulting from Rayleigh photon scattering from the gas sample. The shape of the prompt signal and FWHM of 300 psec. are characteristic of the synchrotron radiation pulse.
- Figure 5. TOF photoelectron spectrum of the 5p shell of atomic Xe.

Figure 6. Schematic for the routing electronics to be used for the measurement of photoelectron angular distributions with two TOF analyzers. CFD = constant fraction discriminator. FI = multiple input fan-in. R = router; this component routes the coincidence pulse-height signal resulting from one of the TOF analyzers and the beam signal to the appropriate storage subgroup of the multichannel analyzer. TAC = time-to-amplitude converter. PHA/MCA = combination pulse-height analyzer and multichannel analyzer.



XBL 792-8566

Figure 1



XBL 7810-11701A

Figure 2

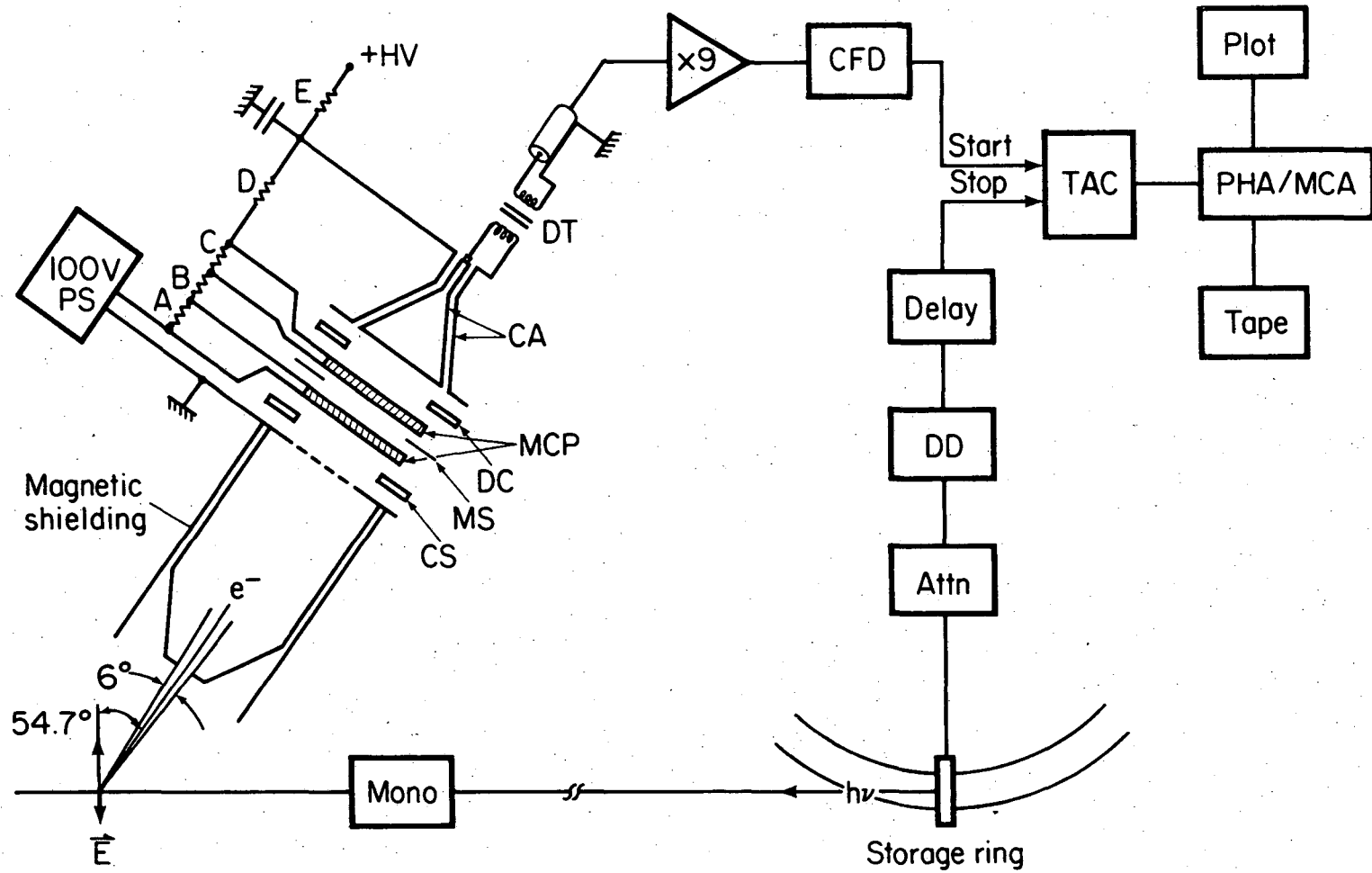
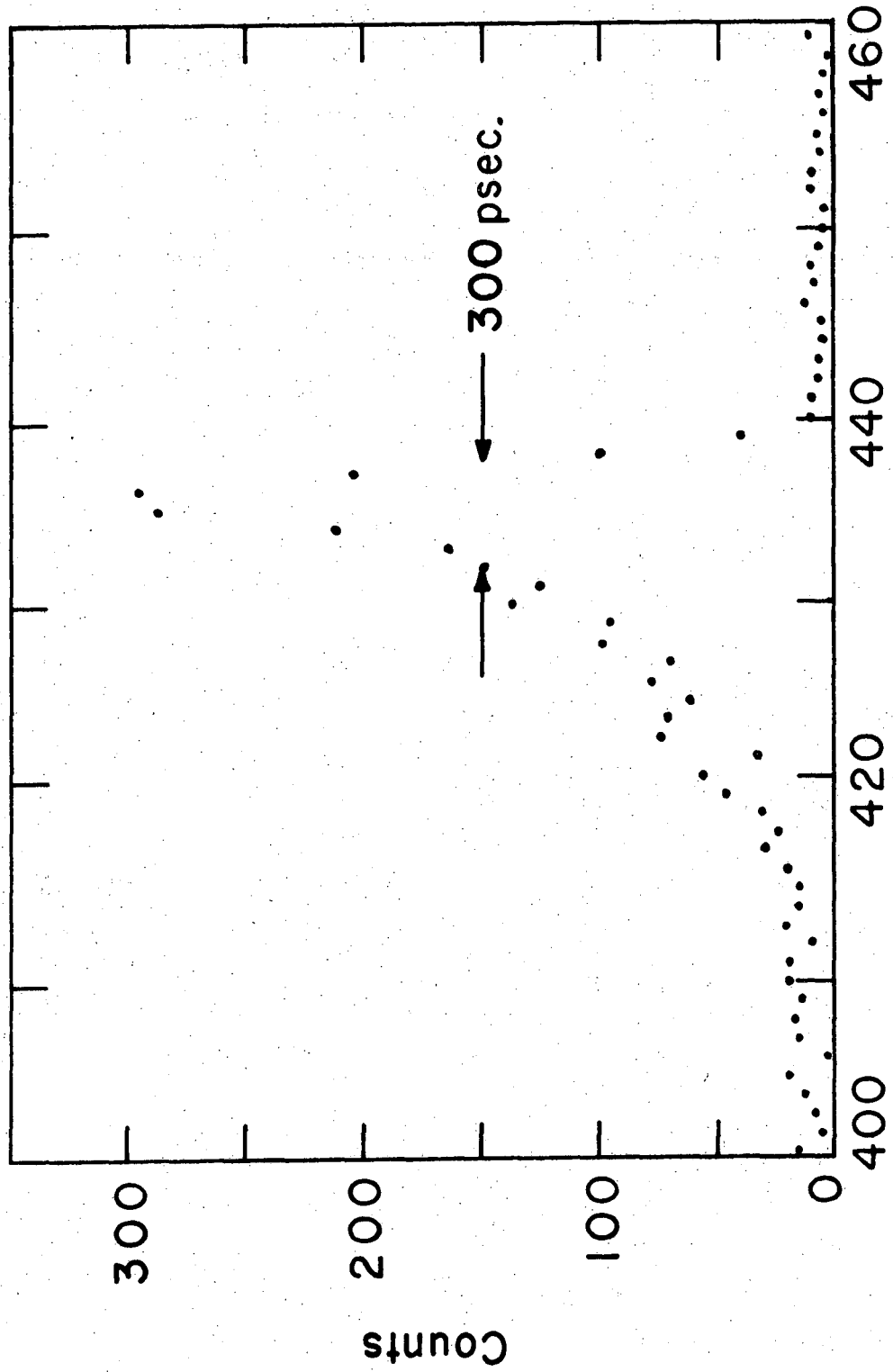


Figure 3

XBL 792-619



Channel Number

XBL 792-8565

Figure 4

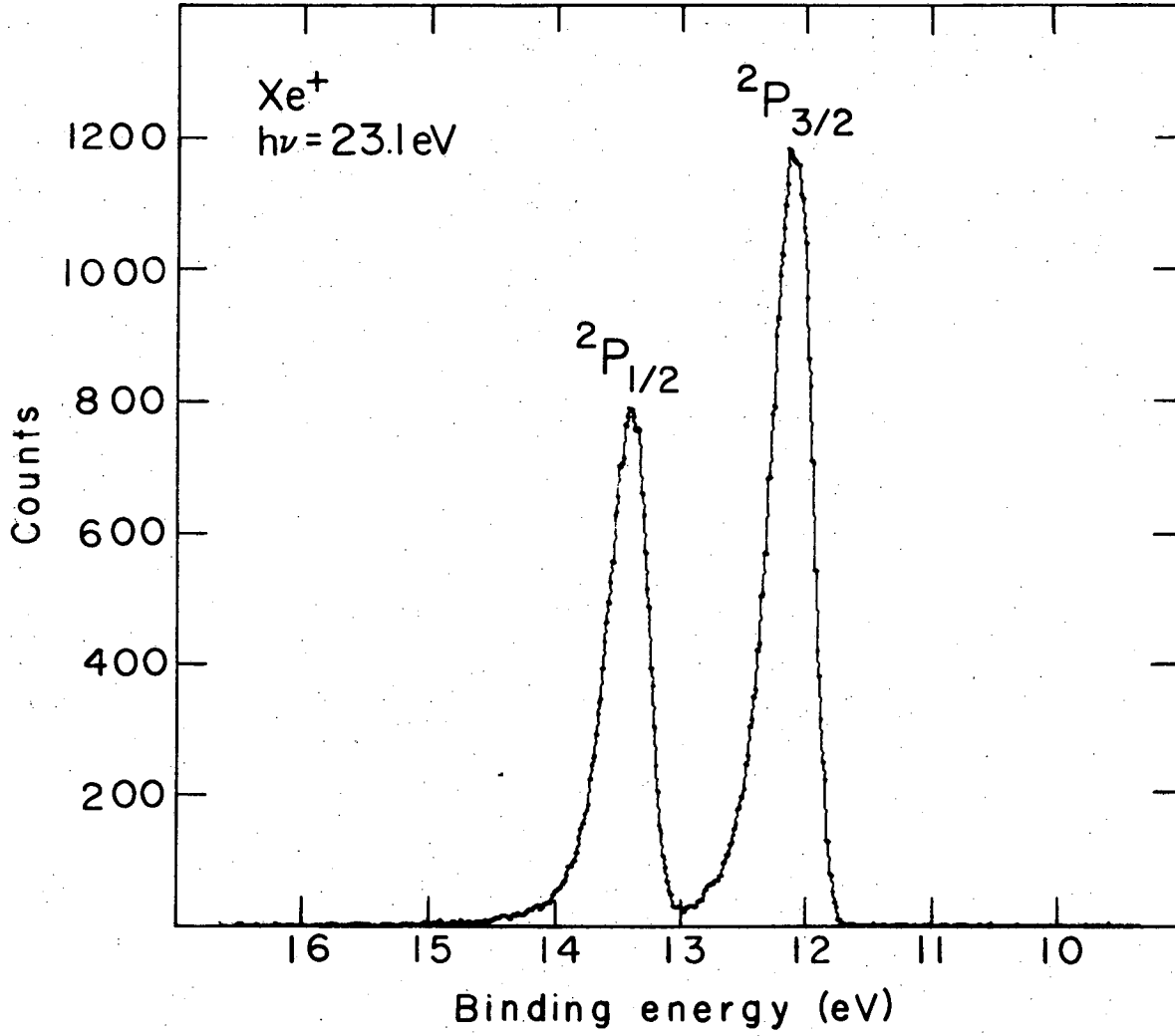


Figure 5

XBL 789-10742A

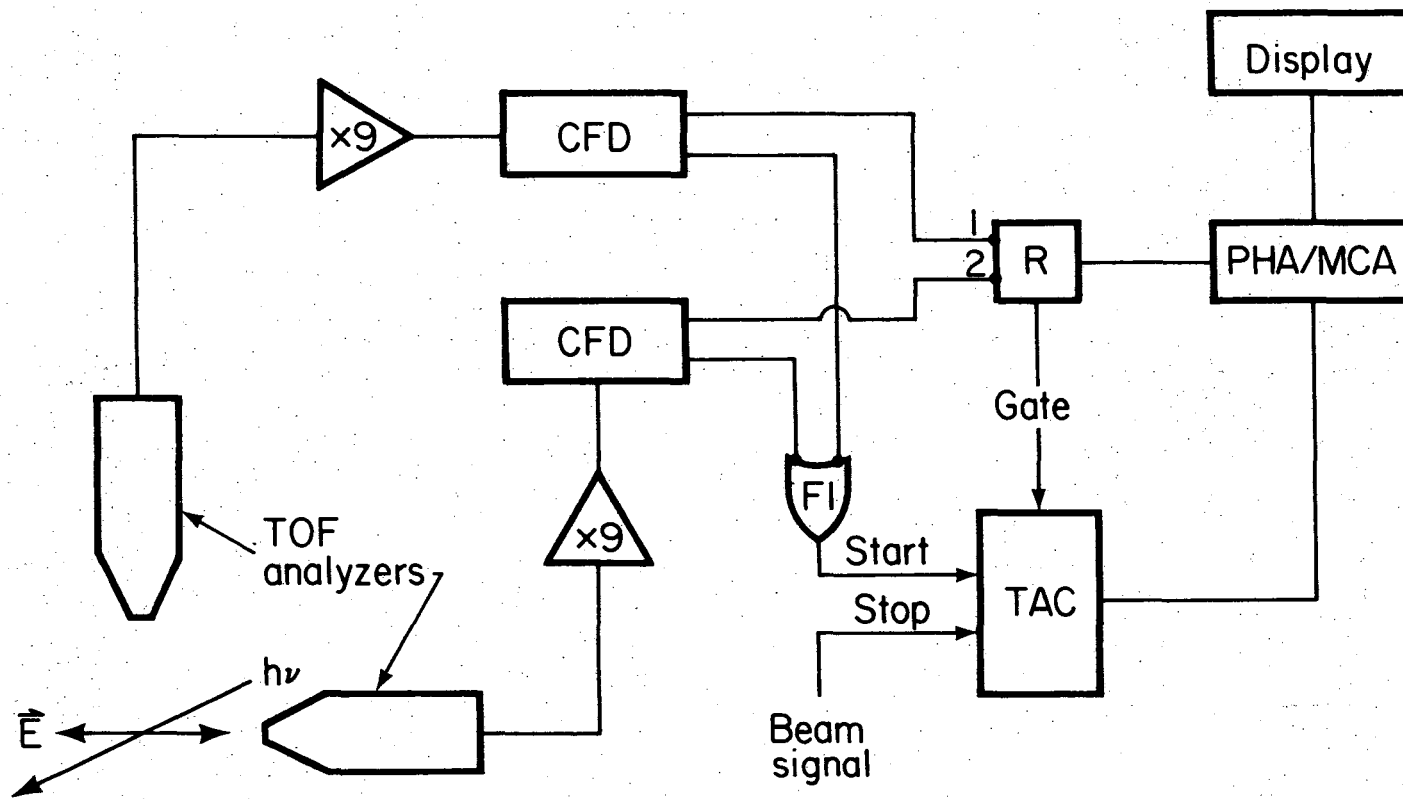


Figure 6

XBL 792-618

This report was done with support from the Department of Energy. Any conclusions or opinions expressed in this report represent solely those of the author(s) and not necessarily those of The Regents of the University of California, the Lawrence Berkeley Laboratory or the Department of Energy.

Reference to a company or product name does not imply approval or recommendation of the product by the University of California or the U.S. Department of Energy to the exclusion of others that may be suitable.

TECHNICAL INFORMATION DEPARTMENT
LAWRENCE BERKELEY LABORATORY
UNIVERSITY OF CALIFORNIA
BERKELEY, CALIFORNIA 94720